Guess heat transfer coefficient of forced convection for single-phase flow in a single-phase passage on a vertical tube heat transfer

R.SHAKIR [1]

Department of Petroleum and Gas engineering,University of Thi-qar- College of engineering, Thi-qar,Iraq
ORCID No: https://orcid.org/0000-0001-5413-0861

Keywords

forced convection, laminar zone, turbulent zone, single-phase to coefficient of heat transfer for single-phase passage.

Abstract

Forced convection is difficult to apply to smooth, vertical circular tubes because very low heat fluxes are needed to prevent buoyancy effects from increasing the heat transfer coefficient. Previous research has mainly focused on mixed convection for both laminar and turbulent zones, with limited study conducted on forced convection for heat transfer. The goal of this study was to investigate the heat transfer coefficient characteristics under specific conditions of forced convection, using smooth circular test sections with both upward and downward flows. Water with a Prandtl number of (6.30-7.10) was used for Reynolds numbers ranging from (490.70 to 17219.95), heat fluxes between (0.510-5.01 kW/m^2) were employed and fluid mean velocities of (0.10 to 3.75) meters per second. Heat inputs between (20 – 200)watts were used during the tests.The width of both the laminar and turbulent flow zones in the fully developed zone and developing turbulent zone were determined for all heat fluxes.

Research Article
Submission Date : 14.04.2023
Accepted Date : 04.05.2023

1. Introduction:

The tube can experience either forced or mixed convection when the flow is laminar. It is crucial to differentiate between these two types of convection due to the significance of Reynolds number under various conditions. Buoyancy effects on the liquid cause density to vary radially in mixed convection. Both forced and mixed convection can occur in laminar convective flow through a tube, and distinguishing between them is important because of the Reynolds number's criticality in different conditions. Buoyancy effects on the liquid cause density to vary radially in mixed convection. Several textbooks on heat transfer, including references (Bejan, 2013), (Ya et al., 2015),(Lienhard, 2013),(Holman, 2012), (SevinGumgum NurcanBaykus Savasaneril, 2018) and (M.Alpbaz, 1988) are proceeded method for the 2-D heat equation so the method converts the 2-D heat equation to a matrix equation that was purpose of this study and the origin of the equation for heat transfer interfacial cofficient by their tests.In the absence of empirical data from practical experiments, the study relied solely on predictive analysis using heat transfer equations for hypothetical setups resembling real-world lab tests conducted under the same circumstances.In the absence of empirical data from practical experiments, the study relied solely on predictive analysis using heat transfer equations for hypothetical setups resembling real-world lab tests conducted under the same circumstances.R.Shakir (R.SHAKIR, 2022a, 2022b; Shakir, 2020, 2021b, 2021a, 2022) conducted a numerical analysis on forced convection in mini-channels with fully developed and developing flows, examining both laminar and turbulent flows under various boundary conditions. And, T. L. Bergman (Bergman et al., 2017) possesses valuable resources in the form of textbooks about heat transfer through heat flow in tubes.,state that under a constant heat flux boundary condition, the Nusselt

*R.SHAKIR; e-mail: raed-sh@utq.edu.iq ; shraed904@gmail.com

number in fully developed and laminar forced convection heat transfer on circular tubes remains constant regardless of the value of the Prandtl number or Reynolds number. The primary aim of this investigation is to devise a sophisticated numerical iterative method that employs a prediction software to establish the properties of forced convection heat transfer and fluid flow.

2. The guess set-up

This paper briefly describes the ideal setup for prediction (illustrated in Figure 1), which includes a closed liquid loop, a test bench structure, an inlet section, a test section, and a low-turbulence section. The inclination of the test section can be adjusted depending on the installation of the test bench. As depicted in Figure 1, the test section produced conditions for forced convection when placed vertically. Water was dispensed from a 600-liter storage tank through flow meters, a flow-calming section, the test section, and then returned to the storage tank for redistribution and cooling.

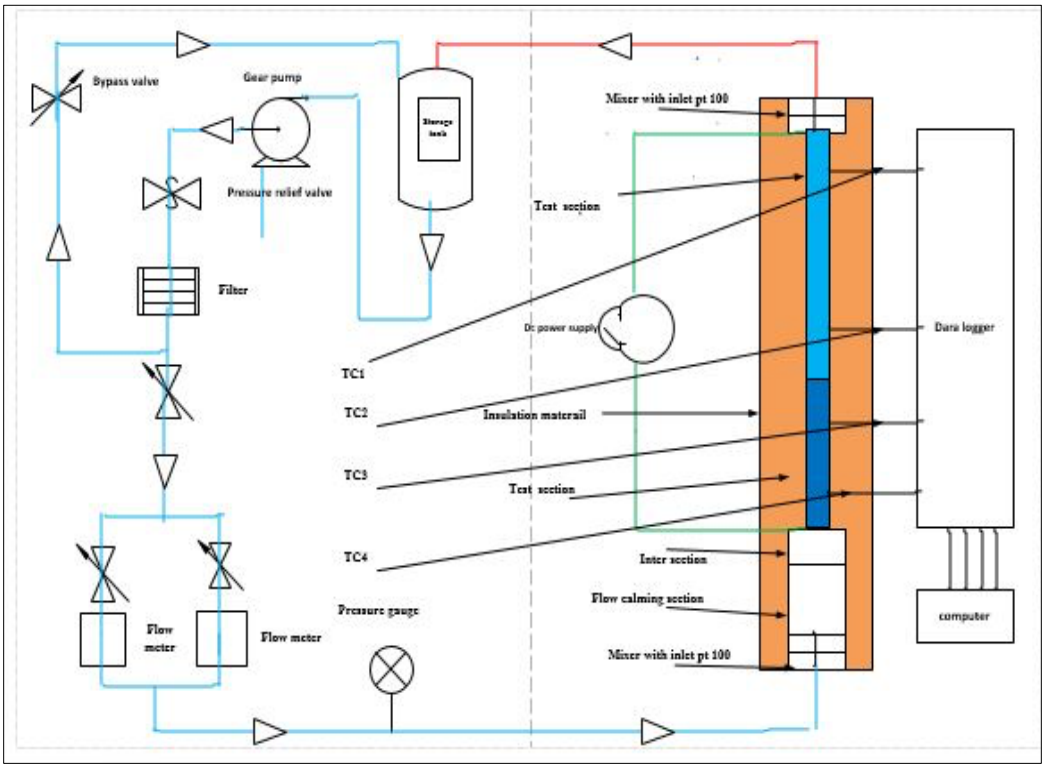

Figure 1.Test section

To maintain a constant temperature and cool down heated water, a chiller unit was connected to the storage tank in the system. A gear pump with a flow rate of 430 liters per hour was used to circulate the water through the test section, and a rubber hosepipe was utilized to prevent vibrations from the pump from affecting the test section. The flow rate of the water was controlled by a personal computer, and a Lab VIEW program was used to adjust the voltage signal to maintain the desired pressure. To prevent flow disturbances, a pressure relief valve was used to bypass the water back to the storage tank. A water bypass line with two flow meters of different capacities was used to increase back pressure.The mass flow rate of the water was measured using two flow meters, one with a flow rate of (330 liters per hou)r and the other with a flow rate of 108 liters per hour. Both flow meters had an accuracy of (±0.07%) of the full scale. The higher flow meter was used to measure the quasi-turbulent and turbulent zones, while the lower flow

meter was used to measure the laminar zone to the quasi-turbulent flow zone. In addition, Pt100 probes were installed downstream of the inlet mixer and outlet mixer, respectively, inside a soft Nylon mesh to measure the water temperature as it flowed axially along the probe.

To ensure a consistent flow rate in the test segment, a flow-calming segment made of a clear acrylic tube with a diameter of 200mm and a length of 620mm was installed before the test segment, as shown in Figure 1. The flow-calming segment also had three air bleed valves located at the top to remove any trapped air.Figure 1 shows a graphic representation of the test segment, including the locations of two pressure taps, four thermocouple stations, and the orientations for upward and downward vertical flows. The test segment was made of a smooth copper tube with an inner diameter of 5mm and an outer diameter of 50mm. It had a length of 5m, resulting in a higher length-to-diameter ratio (x/Di) of 500.

The test section was mounted on a 5.9m long test bench, which was placed on a rigid frame with a height of 2.9m and dampening pads to prevent vibrations from the floor. The test bench was pivotable at the center, allowing for testing in both upward and downward vertical directions. Tightly secured cables kept the test bench upright and rigid, and a grilled inclinometer was attached to the test bench to confirm the test section's inclination angle.To minimize heat transfer to the surroundings, the flow-calming segment, inlet segment, test segment, mixers, and tubes were insulated using an insulation substance with a thermal conductivity of 0.04 W/m.K. The insulation around the test segment had a thickness of 70mm, and the heat loss was estimated using 1-D heat transfer accounts, taking into account the medium's measured wall and outside insulation temperatures and insulation resistance to be less than 3% if possible.

To reach a steady state, a guessable procedure was employed. Steady-state conditions were assumed when there were no significant changes in mass flow rates, energy balance, temperatures, currents, and pressure drop readings, which took about two hours after the first start-up of the day. The lowest mass flow rate was used as the starting point, with the pump velocity adjusted via a Lab view program on a computer lab to reduce flow pulsations. The bypass and provide valves were continuously adjusted to enable the pump to work at higher mass flow rates. Heat fluxes were generated by a DC power supply by stratifying the requested currents and voltages on the system.Guess readings were taken at higher mass flow rate periods in the laminar and turbulent flow zones, but more time (approximately 25-40 minutes) was needed to reach steady-state conditions in the transitional flow zone. Once steady-state was achieved, approximately (390-410) data points were logged at a frequency of (22 Hz), including inlet and exit temperatures, wall and circumference temperatures, mass flow rates, and pressure drops. The water temperature in the storage tank was monitored to maintain a constant temperature in the test segment. All data collected were saved and analyzed using a separate program.

3. Mathematical processes

The fluid temperatures, T(p), at any axial position,

$$T_p = T_{in} + (T_{out} - T_{in}/L)\, x \tag{1}$$

It appears that over (600) heat transfer equations were utilized by Guess software, and then these equations were sent to Excel software using an iterative method. Based on **Figure 2**, Creation concluded that there is only one spot where heat can flow at the interface of the solid and water. The 2-dimensional array is arranged in such a way that it primarily affects the wall line, while the 1-dimensional array is perpendicular to the water flow and the 2-dimensional array is parallel to the water flow. It is necessary for thermal conductivity to adhere to the process illustrated in **Figure 2.** (Shakir, 2020), (Shakir, 2021b).

$$\delta^2 T/\delta y^2 + \delta^2 T/\delta z^2 = 0 \quad (2)$$

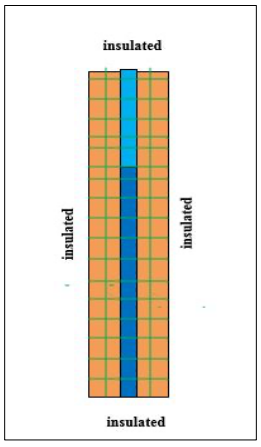

Figure 2.Test segment

The temperature (T) on the copper wall and the perpendicular direction (y) to the axis of water flow were used to obtain the heat transfer in equation (3). This was achieved by dividing the equation by the area of the square cell (0.05 m) squared.(Shakir, 2020), (Shakir, 2021b).

$$T_{i,j} = \delta y^2 \left(T_{i+1,j} + T_{i-1,j}\right) + \delta z^2 \left(T_{i,j+1} + T_{i,j_1}\right)/2\,(\delta y^2 + \delta z^2) \quad (3)$$

To get the area of tube flow,

$$A = \pi {D_h}^2/4 \quad (4)$$

The hydraulic diameter can be found by:-

$$D_h = 4A/P \quad (5)$$

To calculate the fluid of mean velocity by,

$$u = m/\rho\, A \quad (6)$$

To obtain the (Re) by,

$$Re = \rho u D_h/\mu \quad (7)$$

To get the (Pr) by,

$$Pr = C_p \mu/K_f \quad (8)$$

To obtain the (St) by, (Holman, 2012)

$$S_f = E_{st} {R_e}^{-0.205} {P_r}^{-0.503} \quad (9)$$

To obtain the (E-St) by, (Holman, 2012)

$$E_{st} = -0.0225\, exp^{(-0.0225\,(\ln Pr)^2)} \quad (10)$$

To obtain the (Gz) by, (Holman, 2012)

$$G_z = mC_p/K\,L \quad (11)$$

To obtain the (Nu-L) by, (Holman, 2012)

$$Nu = 1.75 G_z^{\frac{1}{3}} \quad (12)$$

To obtain the (Nu-T) by, (Holman, 2012)

$$N_U = 0.023\, R_e^{0.8} P_r^{0.4} \quad (13)$$

To obtain the (h-L) by, [4]

$$h_L = K_C N_u / D_h \quad (14)$$

To obtain the (h-T) by, (Holman, 2012)

$$h_T = \rho\, u C_p S_t \quad (15)$$

4. Results

To examine how buoyancy affects fluid temperatures, **Figure.3** compares temperature data at different heat flux conditions, as a function of Reynolds number, for vertical upward flow in the test section. The figure illustrates that at a heat flux of (3.6, 4.07, 4.6, and 5.10 kW/m^2), the minimum fluid temperature was (20.17, 20.16, 20.15, and 20.14°C), respectively, which was statistically significant, indicating the presence of buoyancy effects that caused flow and mixed convection. This led to a reduction in the Reynolds number with an increase in fluid temperature at the inlet and outlet locations for vertical flow, as well as higher outlet data than inlet data.

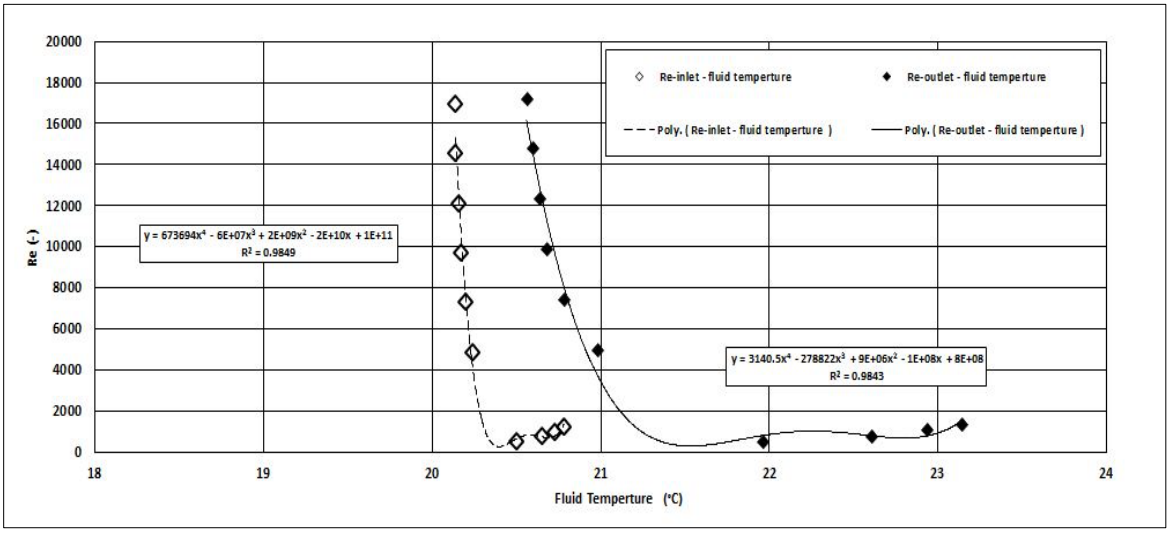

Figure.3. Variation to (Re) versus (Tf)

A correlation was obtained for fully developed laminar and developing turbulent forced convection Reynolds number, which takes into account the increase in Reynolds number with axial location for vertical flow orientation. This correlation was obtained by fitting a simple polynomial curve to all the results for forced convection heat transfer for vertical upward and downward flows (refer to **Figure.4**).

$$Re_{in} = 0.0003(x/D_i)^3 + 0.2955(x/D_i)^2 - 47.53(x/D_i) + 2386.4 \quad (16)$$

$$Re_{out} = 0.0003(x/D_i)^3 + 0.2951(x/D_i)^2 - 47.997(x/D_i) + 2381.8 \quad (17)$$

Equations (16 and 17) hold true for Reynolds numbers ranging from (491-1240) at the inlet data and (518.5-1351.5) at the outlet data, provided that no transition occurs. It is worth mentioning that the onset of transition for vertical tubes typically occurs within the Reynolds number range of (4857.3-16933.3) at the inlet data and (4998.7-17214.95) at the outlet data. This range of Reynolds numbers is significantly influenced by the heat flux, tube diameter, and inlet geometry. Thus, the equations accurately depict the dependence of laminar and turbulent forced convection heat flow on Reynolds number along the length of the tube in the entrance zone.

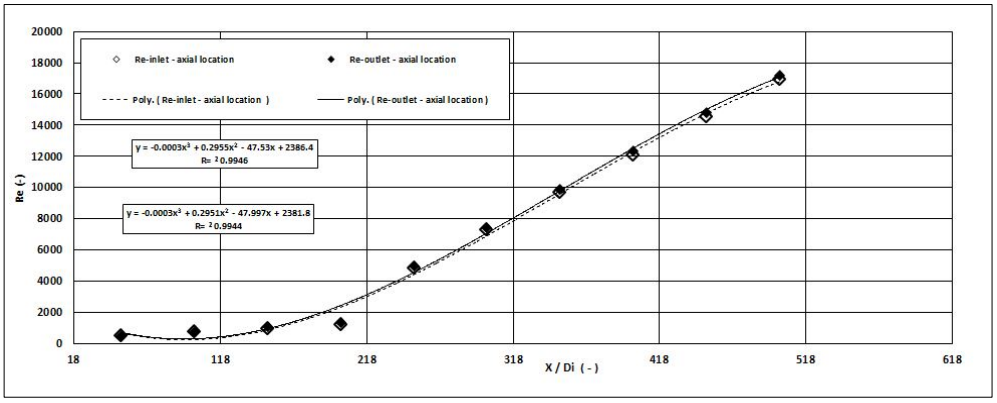

Figure.4. Variation to (Re) as a function of axial location

The coefficient of heat transfer varies with the mass flow rate for different heat fluxes, as shown in **Figure.5.** The data in **Figure.5** reveals that when the mass flow rate is fixed at values of (0.002, 0.003, 0.004), and (0.005) kg/s, an increase in heat flux leads to an increase in the coefficient of heat transfer. Moreover, for mass flow rates higher than (0.005 kg/s), the coefficient of heat transfer increases slightly in a polynomial relationship as the mass flow rate increases. This information is evident from the data presented in **Figure.5**.

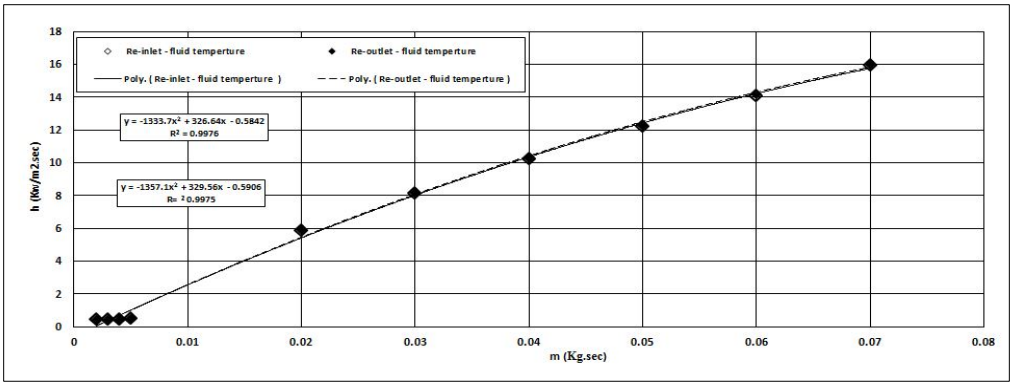

Figure.5. Variation of coefficient of heat transfer as function rate of mass flow

Figure.6. illustrates a comparison between the laminar Reynolds numbers for forced and mixed convection, under different heating conditions and rates of mass flow. The results show that, for vertical flow, the average Reynolds number was approximately the same for all heat fluxes (ranging from 0.510 to 2.04 kW/m^2) at the inlet and outlet locations. However, the forced convection Reynolds number did not fully develop and was not constant at (2.55 kW/m^2) and beyond. Instead, it slightly increased as the rate of fluid velocity increased for all heat fluxes, following a power relationship.

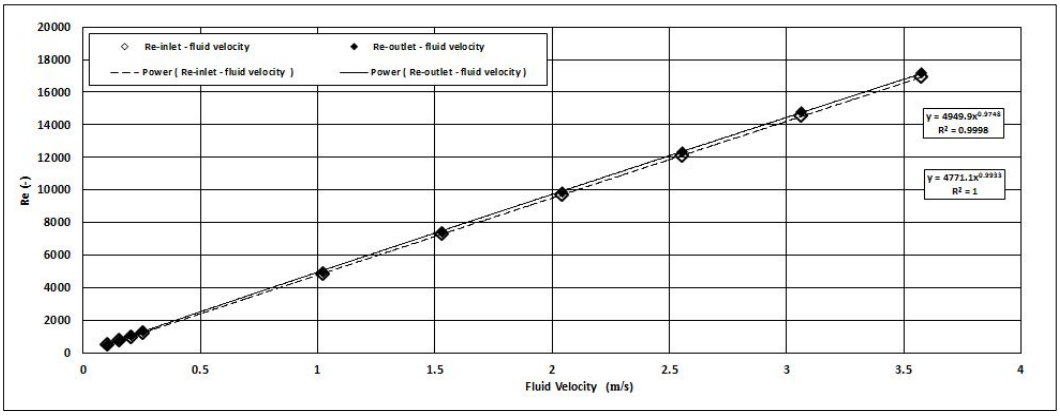

Figure.6. Variation of coefficient of heat transfer as function rate of mass flow

5. Conclusions

Previously, there has been limited research on forced convection in both the laminar and turbulent zones. To ensure that forced convection and buoyancy effects were minimized, experiments were conducted in both upward and downward directions. The value of (Reynolds number) at which the transition from laminar to turbulent flow occurred increased with increasing heat flux in both the fully developed and developing zones. To conduct uncertainty analysis in this paper, it is recommended to increase the (Reynolds number) by increasing the heat flux, which in turn increases the temperature and reduces viscosity. The onset of laminar flow and the cessation of turbulent flow in the fully developed region occurred at higher Reynolds numbers as the heat flux increased for pure forced convection conditions. Additionally, the width of the flow regime varied for different heat fluxes. Equations were derived to establish the boundaries of the laminar, transitional, and turbulent flow regimes for pure forced convection. The findings revealed that the transition occurred at different mass flow rates for all heat fluxes, similar to the isothermal flow case. Nevertheless, the Reynolds numbers increased as the heat flux increased, which was attributed to the reduction in viscosity as the temperature increased.

Nomenclature

A	area of tube flow (mm2)
Cp	specific heat of water,(kJ/(kg .K)
Dh	hydraulic diameter, mm
E-st	factor of Stanton number (-)
Gz	Graetz number (-)
hL	laminar coefficient of heat transfer, (W/(m2.K)
hT	turbulent coefficient of heat transfer, (W/(m2.K)
Kf	thermal conductivity of fluid, (W/(m .K)
Kc	thermal conductivity of copper, (W/(m .K)
L	tube length (m)
m	mass water flow rate,(kg/s)
Nu	Nusselt number (-)
Pr	Prandtl number (-)
St	Stanton number (-)
Re	Reynolds number (-)
T	temperature,(K)

V	water velocity,(m/sec)
ρ	water density, (Kg/m2)
μ	dynamic velocity (N s/m2)

Conflict of Interest

The author's involvement in this study was completely free from any conflicts of interest. There has been no receipt of financial support, and there are no circumstances that would result in financial or personal gain.

References

Bejan, A. (2013). Convection heat transfer. John wiley & sons.

Bergman, T. L., Incropera, F. P., & DeWitt, D. P. (2017). Fundamentals of Heat and Mass Transfer; Bergman, TL, Lavine, AS, Eds. John Wiley & Sons, Inc.: Hoboken, NJ, USA.

Holman, J. P. (2012). Heat Transfer (ten editio). McGRAW-HILL'S.

Lienhard, J. H. (2013). A heat transfer textbook: Courier Corporation. Massachusetts Institute of Technology.

M.Alpbaz. (1988). THE ORIGIN OF THE EQUATION FOR THE İNTERFACİAL COEFFICIENT OF HEAT TRANSFER. Journal, 34(01.02), 114–128.

R.SHAKIR, R. S. (2022a). Investigate the Flow of Boiling Heat Transfer in a Complex Geometry Flat Channel. University of Thi-Qar Journal for Engineering Sciences 25–21 ,(1)12 ,مجلة جامعة ذي قار للعلوم الهندسية.

R.SHAKIR, R. S. (2022b). Pressure Drop Effect on Mini-Scale Heat Sink by Multi-phase: Review & Prediction. University of Thi-Qar Journal for Engineering Sciences ,(1)12 ,مجلة جامعة ذي قار للعلوم الهندسية 20–15.

SevinGumgum NurcanBaykus Savasaneril, E. (2018). Chebyshev collocation method for the two-dimensional heat equation. Journal, 3(2), 1–8.

Shakir, R. (2020). Boiling Heat Transfer in a Micro-Channel Complex Geometry. IOP Conference Series: Materials Science and Engineering, 928(2), 22129.

Shakir, R. (2021a). INVESTIGATION OF SINGLE-PHASE FLOW CHARACTERISTICS IN A STAGGER PIN-FINS COMPLEX GEOMETRY. Journal of Engineering and Sustainable Development, 25(6), 74–81.

Shakir, R. (2021b). Investigation of Single-Phase Flow Characteristics in an Inline Pin-Fins Complex Geometry. Journal of Physics: Conference Series, 1879(3), 32118.

Shakir, R. (2022). Study Of Pressure Drop and Heat Transfer Characteristics Of Mini-Channel Heat Sinks. The Iraqi Journal for Mechanical and Materials Engineering, 22(2), 85–97. https://doi.org/10.32852/iqjfmme.v22i2.595

Ya, C., Ghajar, A., & Ma, H. (2015). Heat and Mass Transfer Fundamentals & Applications. McGraw-Hill.